11-20-2001

Condensation of Carbon in Radioactive Supernova Gas

Donald D. Clayton
Clemson University, claydonald@gmail.com

Ethan A-N. Deneault
Clemson University

Bradley S. Meyer
Clemson University

THE ASTROPHYSICAL JOURNAL, 562:480–493, 2001 November 20

CONDENSATION OF CARBON IN RADIOACTIVE SUPERNOVA GAS

DONALD D. CLAYTON, ETHAN A.-N. DENEAULT, AND BRADLEY S. MEYER
Department of Physics and Astronomy, Clemson University, Clemson, SC 29634-0978
Received 2001 April 26; accepted 2001 July 24

ABSTRACT

The chemistry of carbon molecules leading to the formation of large carbon-bearing molecules and dust in the interior of an expanding supernova is explored and the equations governing their abundances are solved. A steady state between production and destruction is set up early and evolves adiabatically as the supernova evolves. Simple solutions for that steady state limit yield the abundance of each linear carbon molecule and its dependence on the C/O atomic ratio in the gas. Carbon dust condenses from initially gaseous C and O atoms because Compton electrons produced by the radioactivity cause dissociation of the CO molecules, which would otherwise form and limit the supply of C atoms. The resulting free C atoms enable carbon dust to grow faster by C association than its destruction by oxidation for various C/O ratios. Nucleation for graphite growth occurs when linear C_n molecules transition to ringed C_n molecules. We survey the dependence of the abundances of these molecules on the C/O ratio and on several other kinetic rate parameters. The concept of "population control" is significant for the maximum sizes of carbon particles grown during supernova expansion. Interpretation of presolar micrometer-sized carbon solids found in meteorites and of infrared emission from supernova is relaxed to allow O to be more abundant than C, but the maximum grain size depends upon that ratio.

Subject headings: astrochemistry — dust, extinction — infrared: stars — molecular processes — radiative transfer — supernova remnants

1. INTRODUCTION

The goal of this study is to understand the abundances of linear-chain carbon molecules within expanding supernova interiors. Those interiors are hydrogen free, so the chemistry is dominated by carbon and oxygen atoms. Oxidation by free O atoms opposes the association of free carbon into carbon clusters. Linear chains of n carbon atoms, called C_n, grow to lengths $n = 10$–24 before spontaneous isomerization renders them cyclic. Their abundances are stepping stones to the growth of larger carbon solids subsequent to that isomerization. In that sense the cyclic C_n are nuclei for the growth of carbon dust in the supernova's expanding and cooling interior. Their abundances determine the rate of association of free C atoms in the flow toward larger particles. And they set the abundance level of all that is to follow.

Our kinetic approach differs from that of equilibrium nucleation theory. The abundances of the linear molecules C_n are established in a steady state between creation and destruction, but that steady state differs greatly from the thermal equilibrium steady state because of the large departure from equilibrium of the abundance of the CO molecule. A later section devotes its attention to clarification of this distinction among steady states.

Astronomical significance follows directly from the recovery of these supernova particles from meteorites and from their redistribution of the supernova light curve (see below). The novelty of the chemistry is generated by the breakup owing to radioactivity of the CO molecule, which normally is thought to lock up the lesser of the C and O abundances at an early stage of an equilibrium cooling sequence. Because the supernova interior is so oxidizing in most of its mass, this point is essential to understanding the growth of supernova graphite grains. The point has been demonstrated by the numerical calculations of Clayton, Liu, & Dalgarno (1999, hereafter CLD99). The present work clarifies the behavior of the reaction network established by CLD99. Were H present, the reaction network would have many more complications (e.g., Pascoli & Polleux 2000).

1.1. *The Radioactive Environment and the* CO *Mass*

Supernovae are profoundly radioactive. For a few years following the explosions, their interiors can be thought of as cooling thermal gases containing a hornet's nest of energetic particles. A graph of the production rate per gram of Compton electrons as a function of their recoil energy is presented (for several different mass zones of a model of supernova 1987A) by Clayton & The (1991). Compton electrons and X-rays are created in this way by the primary gamma rays of the radioactivity, and their interactions with the expanding mass provide various observational displays: their degradation into thermal heat in the gases causes the visual light of supernovae to be emitted; early escape from the supernova surface of hard X-rays created in the final states of Compton scattering events presages the appearance of gamma-ray lines; the escaping gamma-ray lines demonstrate the correctness of explosive nucleosynthesis theory and measure the yield of radioactivity, primarily ^{56}Ni and its daughter ^{56}Co; partial escape of positrons following ^{56}Co decay contributes to the galactic glow at 511 keV; nonthermal radiation from neutrals, ions, and electron-ion recombination is seen emanating from cool gases from which it would be unexpected but for the radioactive excitations; and the growth and survival of molecules and dust is moderated by the X-rays and Compton electrons. All of these and more follow from the realization that supernova interiors are bathed with the suprathermal emanations of radioactive ^{56}Co (Clayton, Colgate, & Fishman 1969; Colgate & McKee 1969; Clayton & The 1991).

Despite the complexity of the supernova phenomenon, the state of internal matter after the first week of violent expansion is well understood and predictable: a gas coasting radially outward having velocity proportional to radial distance, cooled by the work of differential expansion but

heated by predictable transport of gamma rays and X-rays arising from the central ^{56}Co radioactivity. The spectrum and rate of production of fast electrons having energies from tens to hundreds of keV at differing depths has been calculated and displayed by Clayton & The (1991). Their Figures 1 and 2 show that the Compton-electron production spectrum is proportional to $(1 + E/E_0)^{-2}$ and that at $t = 175$ days (a significant epoch for dust growth) the total number rate averaged over the entire model of SN 1987A averages 5×10^{13} g^{-1} s^{-1} and has the value 1.0×10^{14} g^{-1} s^{-1} in the carbon shell (depth $m = 14$). The rate at other time scales with the radioactive power $e^{(-t/111d)}$. These rates for energizing electrons are adequate for computation of their chemical effects. Thus about

$$N_{\rm cre} = 1 \times 10^{14} e^{[-(t-175d)/111d]} \text{ g}^{-1} \text{ s}^{-1} \quad (1)$$

Compton recoil electrons are energized per gram per second within the carbon shell. This means that during 1 yr about 1% of all electrons suffer a Compton collision. An even greater number suffer energizing collisions with those fast Compton electrons, so a large fraction of all electrons suffer an energizing collision during the year (a characteristic time for a supernova). No wonder, then, that their number density at any time (their production rate times their energy-loss lifetime) is adequate to produce serious chemical consequences. In particular, the CO molecule lives only a couple of months before disruption, thereby returning free carbon to the gas.

A series of works (Lepp, Dalgarno, & McCray 1990; Liu, Dalgarno, & Lepp 1992; Liu & Dalgarno 1994, 1995, 1996) have demonstrated the profound consequences of this radioactivity for the formation and survival of molecules. In particular, the chemically inert CO molecule is disrupted shortly after its formation by ionizing collisions with the fast electrons, or by dissociative collisions with fast electrons, or by charge exchange with the He^+ that exists by virtue of the radioactivity. Comparison of the computed and observed masses of CO in SN 1987A is shown by Liu & Dalgarno (1995). The lifetime of a CO molecule is of order months, depending upon the time since the explosion, so its abundance maintains near steady state with respect to its formation and destruction while the interior expands. The energetic particles enable one to understand why the observed CO mass is only a few percent of the much larger mass that would have been present in the absence of radioactivity. Despite the falling thermal temperature of the gas and despite the adequate radiative association rate for $C + O \rightarrow CO$, the calculated CO mass, like the observed estimates, levels off near $5 \times 10^{-3}\ M_\odot$, whereas it would have been perhaps 50 times greater in the absence of radioactivity. Because CO is not a dominant chemical form for C, the remainder of it will be mostly in free neutral C atoms since the radioactivity causes the supernova ejecta to be only lightly ionized (Liu et al. 1992).

A subsequent calculation of the CO mass in SN1987A by Gearhart, Wheeler, & Swartz (1999) differed from that of Liu & Dalgarno (1995) by ejecting only about $10^{-4}\ M_\odot$ of CO, roughly 50 times less than the mass calculated by Liu & Dalgarno (1995). Figure 1 reproduces Figure 7*a* of Gearhart et al. (1999) in order to display the gaseous number densities of C, O, and CO at $t = 200$ days in their model calculation. Although we believe this ejected CO mass to be too small for reasons to be stated below, the calculated CO abundance peaks between 1.5 and 3 $M_\odot$, where the largest density of C atoms exists. For the same reason the mass of carbon solids condensed will also be strongly concentrated in this zone plus that of the C-rich helium-burning shell between 3 and 5 $M_\odot$. Note also in Figure 1 that the C/O abundance ratio changes from less than unity to greater than unity near 3 $M_\odot$; however, if the composition can be mixed at the molecular level before dust condensation (which we doubt), that composition is O-rich everywhere, as shown in Figure 7*b* of Gearhart et al. (1999).

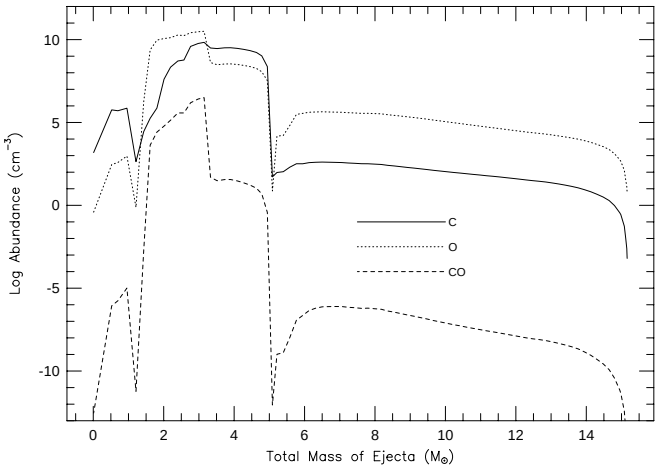

FIG. 1.—Model of SN 1987A reproduces Fig. 7*a* of Gearhart et al. (1999) in order to display the gaseous number densities of C, O, and molecular CO at $t = 200$ days in their model calculation. Although we believe this ejected CO mass to be too small by a factor of 50 for reasons stated in the text, the calculated CO abundance shows that the C atoms are overwhelmingly free. CO abundance peaks between 1.5 and 3 $M_\odot$, where the largest density of C atoms exists. For the same reason the mass of carbon solids condensed will also be strongly concentrated in this zone plus that of the C-rich helium-burning shell between 3 and 5 $M_\odot$.

We believe, based on private discussions with W. Liu and C. Wheeler, that this difference in the calculation of CO mass resulted from an excessively large destruction rate of CO owing to interactions with the O^+ molecule. The O^+ abundance used by Gearhart et al. may have been too large owing to their belief that the destruction of O^+ by charge exchange with atomic C is small. Figure 9 of Gearhart et al. (1999) shows that their calculations find charge exchange with O^+ to be the dominant destruction of CO. However, O^+ should be, we believe, much less abundant because of charge-exchange destruction by neutral C, in which case their CO mass will agree with Liu & Dalgarno (1995). The reader must appreciate that in either calculation the abundance of CO ejected is much less than that of C, so most carbon remains free atoms. The radioactivity (which is responsible for the fast-electron dissociation of CO and also for whatever O^+ does exist) has the effect of nullifying the permanence of the CO trap for atomic C within supernovae. Our study relies on this main point rather than on the precise value of the small CO mass fraction. Our results are valid for either calculation of the small CO abundance, requiring only that almost all carbon remains free of oxidation.

The consequences of having free C atoms for dust growth within the expanding supernova interior are profound. The continuously cooling gases are forced to contain a large abundance of free carbon atoms even though they are accompanied by an even greater number of free O atoms. The vapor pressure of C is made vastly greater than would

be expected in terms of thermodynamic equilibrium at the kinetic temperature of the gas. Such supersaturation of the C vapor is a potential driver of rapid condensation of carbon into solid form. The conventional wisdom, embodied in the statistical equilibrium of slowly cooled gases containing C and O atoms, is that the one of lesser abundance will be consumed in the tightly bound (11.09 eV) CO molecule, which is chemically almost inert, so the chemistry of the remaining gas will be dominated by the greater of the C and O abundances. This paradigm has worked well in understanding the chemistry of asymptotic giant branch star envelopes (Lodders & Fegley 1997; Sharp & Wasserburg 1995), and it has been argued to apply in supernovae as well (Bernatowicz et al. 1996; Amari & Zinner 1997). But the existence of abundant free C atoms, unanticipated in equilibrium theory, within slowly cooled supernova gas has called this into question.

1.2. *Supernova Light-Curve Consequences*

The best evidence of the role of newly condensed dust on the redistribution of radiation from supernovae is derived from observations of SN 1987A, which is our only example of this phenomenon. Major effects of dust condensation observed were a drop in the visual light output after 460 days, blueshifted line profiles after 530 days from the [O I] optical doublet $\lambda\lambda$6300, 6363, and dramatic increase of the IR emission from dust after 500 days. Explanations of these phenomena are reviewed by Wooden (1997), who concludes that dust condensation may have begun as early as 350 days in SN1987A, and by 615 days the dust was so thick that it became optically thick. The 6 month window prior to optical thickness afforded a chance to identify the dust by its spectral features, but none from silicates or SiC could be found. The apparently featureless dust of SN1987A suggests either carbon grains or metallic iron or both. The favored zone for carbon condensation is the C, O core, because it cools the fastest (Wooden 1997) and provides easily the highest density of free C atoms (Fig. 1). Although this zone had been thought sterile in that regard owing to having more O than C, the work of CLD99 changed that outlook greatly. We suggest that the numerous small carbon grains that grow by carbon association after the linear chains isomerize into ringed form provide much of the opacity that SN1987A revealed. Modeling of that opacity must be the topic of a future work, for in this work we address the fundamental chemistry by which these C grains condensed within the O-rich C, O zone.

1.3. *Meteoritic Consequences*

Evidence from meteorites demonstrates that supernova interiors have condensed carbon dust. Both graphite and SiC solids near 1 μm in size have been found within carbonaceous meteorites and extracted for laboratory study (Bernatowicz & Walker 1997). These solids have such widely distinct isotopic compositions in comparison with solar material and with all expectations for interstellar gas compositions that they are easily identified as condensates within gas expelled from stars prior to dilution with surrounding interstellar matter. Of concern here, many are demonstrably supernova condensates (Nittler et al. 1996; Hoppe et al. 1996a; Clayton, Amari, & Zinner 1997; Amari & Zinner 1997). Indeed, their distinguishing isotopic characteristics had been predicted decades earlier (Clayton 1975, 1978), so their isotopic strangeness was less unexpected than was the good fortune of actually finding and extracting them from the meteorites. A large overabundance of daughter ^{44}Ca of 60 yr radioactive ^{44}Ti in some of these supernova particles (Nittler et al. 1996; Hoppe et al. 1996a) demonstrates unequivocally their supernova origin (Clayton 1975). But superimposed on the clear supernova signature is a chemical problem: namely, how does the carbon dust grow within the supernova interior that has far more O than C? For most of the supernova gas, especially interior to the helium-burning shell, the gas is oxidizing.

For almost two decades it has been argued (Clayton 1981) that such carbon grains (at that time still not isolated from the host meteorites) must have condensed only within the gas expanded from the prior He-burning shell of supernovae, because that shell is the only shell wherein the abundance of C exceeds that of O (Fig. 1). But the carbon in that shell is almost isotopically pure ^{12}C, and its silicon is ^{28}Si-poor rather than ^{28}Si-rich. The detailed interpretations of the isotopic ratios measured in the supernova particles have labored under the presumed requirement (e.g., Hoppe et al. 1996b; Hoppe et al. 1996a; Amari & Zinner 1997; Travaglio et al. 1999) that external matter must mix into this ^{12}C-rich shell without increasing the O abundance to a value greater than that of C. The problem faced by this restriction is the set of isotopic ratios measured in these particles (Clayton et al. 1997): both the ^{28}Si-rich Si and the ^{44}Ti are separated by a huge mass of oxygen from that carbon-rich shell, and observed abundances of both the ^{13}C that would ameliorate the ^{12}C purity and the ^{15}N lie in O-rich gas. On the other hand, CLD99's calculations demonstrated that the requirement C/O > 1 does not apply in the supernova environment for reasons reviewed above. The graphite (and other carbon dust) condensation occurs kinetically in the face of a constraint imposed by the energetic particles and by abundant free O atoms. In the supernova during the growth epoch almost all C atoms and O atoms are free, independent of the C/O ratio, so that distinctions between C/O < 1 and C/O > 1 are not appropriate guidelines.

To understand the precursor abundances for carbon grains, it is necessary to understand the abundances of the linear C_n molecule. That is the goal of this work. When n becomes sufficiently large, the linear chain can spontaneously close to a ring. It is the abundances of ringed isomers that provide the seeds for the growth of macroscopic grains. Through the rates of those isomerizations the abundances of linear C_n molecules determine both the abundances and the final sizes of carbon solids.

2. RATE EQUATIONS OF LINEAR MOLECULES

Our chemical network contains many types of chemical reactions for large linear carbon molecules, some of which have been utilized in some recent models of interstellar chemistry (Herbst et al. 1994; Bettens, Lee, & Herbst 1995; Bettens & Herbst 1995, 1996, 1997; Terzieva & Herbst 1998). These reactions and our adopted rate coefficients (Table 1) are the same as the set chosen by CLD99. To them should be added the rate for thermal dissociation of each molecule owing to the ambient temperature and the nonthermal dissociation owing to Compton electrons. We provide an estimate of the former rate from detailed balance below, and we find that below $T = 2000$ K the thermal dissociation of the C_n molecules can be neglected because each one is destroyed more rapidly by chemical reactions

TABLE 1

RATE COEFFICIENTS[a] OF REACTIONS OF LINEAR CARBON CHAINS C_n ($n < 24$)

Reaction	Reactants	Products	k ($cm^3\ s^{-1}$)	n
Equation (8)....	$C + C_{2n-1}$	$C_{2n} + h\nu$	10^{-17}	1
			10^{-10}	>1
Equation (8)....	$C + C_{2n}$	$C_{2n+1} + h\nu$	10^{-17}	1
			10^{-13}	>1
Equation (9)....	$C + C_{2n}$	$C_m + C_{2n-m+1}$	10^{-10}	>1
Equation (14)...	$O + C_{2n+1}$	$CO + C_{2n}$	10^{-12}	1
			10^{-13}	>1
Equation (14)...	$O + C_{2n}$	$CO + C_{2n-1}$	10^{-10}	

[a] Taken from Clayton et al. 1999.

with free atoms. Similarly, the rate of destruction owing to Compton electrons, being comparable to that rate for the CO molecule, is much too slow to compete with chemical destruction of those molecules that are, unlike CO, chemically reactive.

With these rates and the coupled differential equations governing the abundances of the linear-chain carbon molecules, we calculate the evolution of their abundances. Because the molecules are created and destroyed more rapidly than the environment changes, they assume stationary concentrations. These are the first carbon molecules to form in a gas containing abundant free C atoms and O atoms and bathed in the expected fluxes of Compton electrons and X rays, expanding such that its density declines as t^{-3}. We include large carbon molecules and small solids in this picture in order to study the growth of solids. Once small solids exist, they continue to grow if the kinetic reactions of oxidation (destructive) are slower than the kinetic reactions of C association (growth). Viewed that way, the survival of C solids when O > C may then be understood, because the steady bath of free C atoms maintains growth. With the CO trap deactivated, the threat to growth of carbon becomes their oxidation rather than their inaccessibility to condensable C. The competition now is a kinetic one between growth of a carbon cluster C_n by impact with C atoms, where n is the number of C atoms in the grain, and breakup of it by impact with O atoms. Even when the latter are more numerous, kinetic factors can favor growth.

We follow Clayton et al. (1999) in assuming that sufficiently long chains of carbon atoms spontaneously assume ringed structure, which is more stable than the linear chain (Bettens & Herbst 1996). For sake of definiteness, in this work we take that isomerization to occur spontaneously and rapidly when $n = 24$, but the isomerization may occur at significant rates for chains as small as $n = 10$ (Weltner & Van Zee 1989). This uncertainty will assume considerable importance. Once ringed molecules exist, their oxidation rates become much slower and oxidation becomes less a threat as long as abundant free C atoms also exist. Reactions involving these stable ringed molecules should be primarily associative in nature, because oxidation should not proceed rapidly. So C_{24} (or perhaps smaller monocyclic rings) may act as an important seed for rapid growth of larger carbon clusters. Before writing the rate equations governing the abundances of the linear C_n, we next consider their disruption owing to thermal energy of the gas particles. This term was not studied by CLD99 because they chose to consider sufficiently late times and low temperatures that thermal dissociation would be too slow.

2.1. *Thermal Destruction*

The CLD99 equations apply to circumstances for which the temperature is less than 2000 K, which is low enough that thermal decomposition of many molecules can be neglected. This is the case if the destruction rate for each molecule owing to specific reactions greatly exceeds the destruction rate attendant to inelastic collisions in the local thermal bath. That latter destruction rate can be calculated from the abundance ratios that would exist if local thermodynamic equilibrium existed. Consider the molecule C_2 as specific example of this procedure. Statistical equilibrium at temperature T would provide the ratio

$$N_{\rm eq}(C_2) = \left[\frac{G(C_2)}{G(C)^2}\right] N(C)^2 \left(\frac{h^2}{2\pi MkT}\right)^{3/2} e^{B(2)/kT}\ , \qquad (2)$$

where $B(2) = 6.30$ eV is the binding of the C_2 molecule, N is the number density of each, G is the statistical weight, and $M = 6$ amu is the reduced mass. At $T = 2000$ K this gives, neglecting statistical weight factors, the ratio $N_{\rm eq}(C_2)/N(C)^2 = 2.2 \times 10^{-11}$, with N expressed per cm^3. Since the rate of formation of C_2 is $k_C \times N(C)^2$, with the radiative association rate $k_C = 10^{-17}\ cm^3\ s^{-1}$, and since the rate of thermal destruction of C_2 in thermal equilibrium would be given by $N_{\rm eq}(C_2)/\tau$, where τ is the thermal lifetime of C_2, the implied balance yields the lifetime of C_2 to be

$$\tau(C_2) = \left[\frac{G(C_2)}{G(C)^2}\right] \frac{1}{k_C} \left(\frac{h^2}{2\pi MkT}\right)^{3/2} e^{B(2)/kT}\ , \qquad (3)$$

which has the value $\tau(C_2) = 2.2 \times 10^6$ s at $T = 2000$ K owing to thermal effects alone (with partition function ratio set to unity). A C_2 molecule would thus live about a month at $T = 2000$ K before being thermally disrupted. But oxidation destroys C_2 much more rapidly. The reaction with oxygen has the fast rate $k_O = 10^{-10}\ cm^3\ s^{-1}$. Since $N(O)$ is of order $10^{10}\ cm^{-3}$ in the CO shell at $t = 2 \times 10^7$ s, the destruction rate of C_2 owing to oxidation is $k_O N(O) = 1\ s^{-1}$, fully 2.2×10^6 times faster than the thermal destruction rate. Accordingly, we conclude that the thermal destruction rate of C_2 can be neglected for temperatures as low as 2000 K. Oxidation is simply much faster owing to the large kinetic rate and the large abundance of free O.

Similar considerations apply to all linear C_n molecules, although their binding energies are smaller than that of C_2. Thermal dissociation rates neglecting the statistical weight factors at two temperatures are included in Table 2 for the linear-chain molecules, along with other energetic quantities. But first consider the energetics.

2.2. *Heats of Formation*

In a significant work for this problem Bettens & Herbst (1995) have calculated the heats of formation and the molecular symmetries for the linear C_n molecules. They employed calculations using molecular dynamics codes and augmented these with semiempirical scalings to cases where experimental data exists. Table 2 lists their results ΔH_f (kJ $mole^{-1}$) for the heats of formation for those molecules given by their study. These heats of formation are the values of the heat required per mole when C_n is assembled from C in its standard reference state, which is graphite. Because our concern is formation from gaseous C atoms, we need additionally the value of the heat of formation of free C atoms

TABLE 2

ENERGETIC AND THERMAL LIFETIMES

Species	ΔH_f[a]	ΔH[b]	ΔU_{bond}[c]	ΔU (eV)	$\tau_{th}(1500)$[d]	$\tau_{th}(2000)$[d]
C_2.....	817	−613	−606.8	6.30	8.62×10^{11}	2.91×10^{6}
C_3.....	831	−701	−694.8	7.21	1.83×10^{15}	1.06×10^{9}
C_4.....	1052	−494	−487.8	5.06	1.74×10^{1}	6.42×10^{-4}
C_5.....	1081	−686	−679.8	7.06	1.19×10^{11}	9.3×10^{4}
C_6.....	1312	−484	−477.8	4.96	1.44×10^{1}	6.47×10^{-4}
C_7.....	1325	−702	−695.8	7.22	7.10×10^{11}	4.03×10^{5}
C_8.....	1487	−553	−546.8	5.68	5.61×10^{3}	6.32×10^{-2}
C_9.....	1554	−648	−641.8	6.66	1.36×10^{10}	2.28×10^{4}
C_{10}.....	1761	−508	−501.8	5.21	2.12×10^{2}	5.89×10^{-3}
C_{11}.....	1806	−670	−663.8	6.89	1.08×10^{11}	1.17×10^{5}
C_{12}.....	2012	−509	−502.8	5.22	3.02×10^{2}	8.23×10^{-3}
C_{13}.....	2049	−678	−671.8	6.97	2.62×10^{11}	2.41×10^{5}
C_{14}.....	2263	−501	−494.8	5.14	2.01×10^{2}	6.41×10^{-3}
C_{15}.....	2292	−686	−679.8	7.06	6.18×10^{11}	4.83×10^{5}
C_{16}.....	2517	−490	−483.8	5.02	1.02×10^{2}	4.04×10^{-3}
C_{17}.....	2535	−697	−690.8	7.17	1.80×10^{12}	1.13×10^{6}
C_{18}.....	2771	−479	−472.8	4.91	5.01×10^{1}	2.48×10^{-3}
C_{19}.....	2778	−708	−701.8	7.28	5.14×10^{12}	2.58×10^{6}
C_{20}.....	3025	−468	−461.8	4.79	2.43×10^{1}	1.50×10^{-3}
C_{21}.....	3021	−719	−712.8	7.40	1.44×10^{13}	5.82×10^{6}
C_{22}.....	3280	−456	−449.8	4.67	1.07×10^{1}	8.43×10^{-4}
C_{23}.....	3263	−732	−725.8	7.53	4.69×10^{13}	1.46×10^{7}
C_{24}.....	3533	−445	−438.8	4.55	5.05×10^{0}	4.95×10^{-4}

[a] Heat of formation (kJ mole^{-1}) from Bettens & Herbst 1995.
[b] Heat of reaction (kJ mole^{-1}) for carbon association (eq. [5]).
[c] Bond energy change (kJ mole^{-1}) in carbon association (eq. [7]).
[d] Thermal lifetime (s) against carbon dissociation (eq. [3]).

from the reference state, which is $\Delta H_f(\mathrm{C}) = 715$ kJ mole^{-1}. Using this information one can calculate the heat of reaction for

$$\mathrm{C}_n + \mathrm{C} \rightarrow \mathrm{C}_{n+1} , \tag{4}$$

and these quantities are also listed in Table 2. For example, the heat of reaction of C_3 from C_2 and C is

$$\begin{aligned} \Delta H(\mathrm{C}_3) &= \Delta H_f(\mathrm{C}_3) - \Delta H_f(\mathrm{C}_2) - \Delta H_f(\mathrm{C}) \\ &= 831 - 817 - 715 \\ &= -701 \text{ kJ mole}^{-1} . \end{aligned} \tag{5}$$

Negative heats of reaction are exothermic, as these reactions all are. They are exothermic because the C atom is bound to the previous linear chain molecule. To obtain the bond energy, however, one notes from the thermodynamic definition of the enthalpy that its change in a reaction is

$$dH = dU + d(PV) = dU + nRT , \tag{6}$$

where dU is the change in internal energy and n is the increase in the number of moles of gas. For the example reaction $n = -1$ because the entrance channel contains two moles (one of C_2 and one of C) whereas the exit channel contains but one (C_3). The change of internal energy, given for such reactions by $dH + RT$, can be expressed as the sum of the increase of thermal energy ($\frac{3}{2}nRT$) plus the increase of the bond energy dU_{bond}. Using $RT = 2.48$ kJ mole^{-1} at $T = 298$ K (standard reference temperature of 25 C) we find that the bond energy

$$dU_{bond} = dH + \tfrac{5}{2}RT = dH + 6.2 \text{ kJ mole}^{-1} . \tag{7}$$

For the example forming C_3 this gives $dU_{bond}(C_3) = -695$ kJ mole^{-1}. Using the useful conversion factor that 100 kJ mole^{-1} = 1.038 eV atom^{-1} yields the separation energy of C from C_3 to be 7.21 eV, which is greater than the dissociation energy of C_2, 6.30 eV. These separation energies are also listed in Table 2. They are the quantities used to calculate the thermal separation rates for the molecules. For those C_n molecules not given by Bettens & Herbst (1995), we interpolate the separation energies based on the systematics of those that they did calculate. These separation energies become as small as 5 eV for C_{2n}; therefore, their thermal dissociation will remain of significance for the longest time during the expansion and cooling.

A theoretical problem exists if the thermal dissociation time calculated as we have becomes shorter than the rate at which the molecules can actually be heated. Destruction rates by particles (association or oxidation) are already operating at the kinetic limit $k = 10^{-10}$. It is doubtful, therefore, that molecules can actually be heated in less than 1 s, which is their destruction time to other causes. To not be taken too far afield in this study, we therefore restrict our analysis to temperatures low enough that the thermal dissociation times are not less than 1 s. Further study of this point becomes a study of its own, whereas we pursue our goal of understanding the kinetic flow at low temperature, taken by us to mean $T < 2000$ K.

2.3. *Main Chemical Reactions*

In the dense, primarily neutral gas of the supernova ejecta, the carbon molecules grow successively via repeated radiative associations with C atoms,

$$\mathrm{C} + \mathrm{C}_{n-1} \rightarrow \mathrm{C}_n + h\nu . \tag{8}$$

Their heats of reaction and bond energies are given in Table 2. Although reaction (8) is slow with a typical value of the rate coefficient around 10^{-17}cm^3 s^{-1} for the radiative production of small molecules such as C_2 and C_3, its rate coefficient increases rapidly for larger molecules because their numerous vibrational modes absorb and distribute the collision energy so that it rarely accumulates in a dissociative channel (Freed, Oka, & Suzuki 1982). Thus the larger chains do not have to radiate immediately to conserve energy, but instead simply exist in states of high excitation to be stabilized eventually by photon emission. This greatly increases the association rate k_C. See also Curl's (1993) discussion of the production of C_6 by the $C_3 + C_3$ reaction, although we will show below that this reaction is not competitive for the lower density supernova kinetics. For even total n we take reaction (8) to be fast, $k_C = 10^{-10}$ cm^3 s^{-1}. However, the time required for radiative association may exceed the lifetime against a competing channel of deexcitation, in which case radiative association will proceed at an effectively slower rate. Reaction (8) may, for example, be slowed down (Bates 1983) in the presence of these competing exothermic channels,

$$C + C_{n-1} \rightarrow C_m + C_{n-m}\,, \tag{9}$$

unless these reactions are slowed either by sizable exit barriers that are larger than the thermal energies of the molecules or by spin barriers associated with the electron symmetry. We call these "fission reactions" and designate their rates by k_f. For the linear carbon chains with their thermochemical properties and molecular states listed in Bettens & Herbst (1995), reaction (9) is exothermic for odd total number of C atoms in the entrance channel and may proceed rapidly. But for even total number of C atoms, the fission reaction either is endothermic (two even fragments) or involves a change in the total electronic spin of the molecular system, so it may have a large energy barrier. We follow CLD99 in neglecting fission for even total number of C atoms. Because the fission reaction is fast for odd total number, the radiative association reaction proceeds only slowly for odd number but rapidly for even total number. We follow CLD99 by assuming typical values of rate coefficients of 10^{-13} and 10^{-10} cm^3 s^{-1}, respectively. Since we designate rate factors by giving as their arguments the target nucleus rather than the total number of C atoms in the entrance channel, the above implies that we take $k_f(2n)$ to be the larger value and $k_C(2n)$ to be the smaller branch. The fission reaction not only destroys C_n but creates two smaller molecules C_m and C_{n-m}, where m is any integer value between 2 and $n - 1$. The exact distribution of fission fragments is not known, so we will normally take them to be equally distributed among all pairs of final molecules. The significance of that assumption will be tested below. More important is the observation that each fission produces two smaller molecules; accordingly, the effect of the fission reactions will be to increase the total number of molecules, for some sets of rates faster than they can be created by association. For these rates, no steady state would exist; however, the rate set adopted by us does have a steady state. Nonetheless, the effect of doubling will be demonstrated by an example below in which the fission causes larger steady state abundances than would exist if there were no fission reactions at all.

The heats of formation from Table 2 allow an immediate test of whether the fission reactions are exothermic. Consider the example

$$C + C_6 \rightarrow C_4 + C_3 \tag{10}$$

for which the heat of reaction is given by

$$\begin{aligned}\Delta H &= H_f(C_4) + H_f(C_3) - H_f(C_6) - H_f(C)\\ &= 1052 + 831 - 1312 - 715\\ &= -144 \text{ kJ mole}^{-1},\end{aligned} \tag{11}$$

which is negative, showing that heat is given off (exothermic). Because the gaseous mole number is unchanged, moreover, this heat of reaction represents the change in bond energy. Similar calculations show that when the target C_n has odd n, the reaction is endothermic for cases when the fission is into two even-n fragments; thus we take those reactions to occur at negligible rate. For the fragmentation into two odd-n C_n fragments however, the reaction is exothermic. But in these cases the electron spin must change, and we follow CLD99 in assuming that will make the reaction slow enough to be neglected. The spin inhibition can be illustrated by this example:

$$C + C_7 \rightarrow C_5 + C_3\,. \tag{12}$$

Recalling that the C atom is an electronic triplet $S = 1$ in its spin pairing, and referring to the ground-state configuration (Bettens & Herbst 1995), this example reaction can be written

$$(S = 1) + (S = 0) \rightarrow (S = 0) + (S = 0)\,. \tag{13}$$

which clearly requires electron spin flip to occur. Thus we neglect it for purposes of the present study. Summarizing these rate characteristics we follow CLD99 in taking k_C to be small (10^{-13} cm^3 s^{-1}) for even-n targets because k_f is large (10^{-10} cm^3 s^{-1}); conversely for odd-n targets we take k_C to be large (10^{-10} cm^3 s^{-1}) because k_f is small (10^{-13} cm^3 s^{-1}).

Once synthesized, a linear carbon chain C_n is destroyed not only by atomic carbon, either via radiative association or by fissioning, but also by reaction with free oxygen atoms:

$$O + C_n \rightarrow CO + C_{n-1}\,. \tag{14}$$

Reaction (14), although exothermic, is slow for $n = 3$ due in part to the existence of an energy barrier of about 0.1 eV (Woon & Herbst 1996). It may be slow for other odd n (Herbst & Dunbar 1991) with a typical rate coefficient of 10^{-13} cm^3 s^{-1}, but for even n it is probably rapid with a typical rate coefficient of 10^{-10} cm^3 s^{-1} (Terzieva & Herbst 1998), approaching its collisional limit. We will show below that the exact rate for odd n is not important as long as it is less than the rate of C association by odd-n C_n.

It is important to avoid a common misconception by being warned that although the energetic electrons are the major source of destruction of the CO molecule owing to its chemical inertness against reactions with atoms, they do not cause competitive destruction of more reactive molecules. Each chain molecule C_2 is destroyed more rapidly by chemical reactions than by fast electrons. For this reason the Compton electrons play no major role other than that of destroying the CO molecule.

We designate differing reaction types by subscript on the rate factor: k_C for C association; k_O for oxidation; and k_f for fission reactions of even-n linear molecules. Writing the target molecule as the argument of the rate coefficient, the

destruction rate per unit volume for C_n owing to the reaction $C_n + O \rightarrow C_{n-1} + CO$ would be written $k_O(n)N_n N_O$. With this set of reactions we write the equation for the rate of change of C_n.

2.4. *The Growth Equations*

The relevant species for the simplest set of chemical reactions in a cooling gas of C and O atoms are taken to be these: linear C-chain molecules C_n for $2 < n < 24$; cyclic C molecules (ringed) for $n \geq 24$ and for some $n < 24$ at which isomerization is sufficiently rapid; the CO molecule, whose small abundance does not influence the carbon budget except at the exhaustion of free carbon; and carbon solids for larger particles. The last may begin as bicyclic and tricyclic rings, grow into fullerenes, and ultimately into solids that we take to be graphite (Hunter et al. 1994; von Helden, Gotts, & Bowers 1993). The time dependence of the abundance of C_n has positive terms from the C association by C_{n-1} and from oxidation of C_{n+1}. It is also produced as fission fragments of the chain $C_{n'}$ when $n' > n + 1$ and when n' is even. Let the fraction of fission reactions of $C_{n'}$ that results in a fragment C_n be designated by $b_{n(n')}$. Then the equation expressing the rate of change of the N_n abundance reads

$$\frac{dN_n}{dt} = N_C[k_C(n-1)N_{n-1} - k_C(n)N_n - k_f(n)N_n] + N_O k_O(n+1)N_{n+1} - N_O k_O(n)N_n + N_C \sum [k_f(n')N_{n'} b_n(n')] - \frac{N_n}{\tau_{th}} - \frac{N_n}{\tau_e}, \quad (15)$$

where τ_{th} is the thermal dissociation lifetime of C_n and τ_e is its fast-electron lifetime at low temperature. These final two nonchemical dissociation lifetimes are longer than the lifetimes against chemical destruction by either free C or free O except at high temperature; accordingly, the final two destruction terms are omitted in the analysis to follow, but the effect of the first will be returned to later. This repeats the simplification made by CLD99.

Because the abundance N_n changes very slowly in comparison with its chemical destruction time, its value takes on a steady state value $dN_n/dt = 0$. By factoring out the oxygen abundance N_O, this equation for all but C_2 even-n chains can be expressed, for low T, in terms of the C/O abundance ratio:

$$0 = \left(\frac{C}{O}\right)\left[k_C(n-1)N_{n-1} - k_C(n)N_n + \sum_{k=1}^{11-n/2} k_f(n+2k)b_n(n+2k)N_{n+2k} - k_f(n)N_n\right] - sk_O(n)N_n + k_O(n+1)N_{n+1}. \quad (16)$$

For the special case $n = 2$ fission does not appear, whereas production of C_2 from free C atoms must be included.

For the odd-n C_{2n+1} the corresponding equation is

$$0 = \left(\frac{C}{O}\right)\left[k_C(n-1)N_{n-1} - k_C(n)N_n + \sum_{k=0}^{11-(n+1)/2} k_f \times (n+1+2k)b_n(n+1+2k) \times N_{n+1+2k}\right] - k_O(n)N_n + k_O(n+1)N_{n+1}. \quad (17)$$

The difference in these two equations reflects the fact that the fission rate is taken to be zero for odd-n chains C_n and that the sums appearing in the creation as fission fragments are therefore written with slightly different indexing.

These two steady state equations can be written in a 24×24 matrix equation

$$[(1 - \hat{F}^T)\hat{L}]\hat{Y} = \hat{P}. \quad (18)$$

where the elements of $\hat{F}_{ij}$ are the fraction of the destruction of i leading to j, $\hat{L}$ is a diagonal matrix containing the total destruction rates of C_i, the abundance vector $\hat{Y} = [C_2, C_3, C_4, \ldots, C_{24}]$, and where $\hat{P}$ is the production vector, which is zero except for production of C_2 in the first line from free C atoms, which themselves lie outside the components of the vector. Although many techniques exist for solving such matrix equations, we have used an approach devised by Gupta & Meyer (2001). This method's graph-theory applications are very powerful for solving other questions that we intend to pursue in subsequent work. In all results to be presented, we confirmed that the matrix solutions are correct by direct substitution into the matrix equation to confirm that it is satisfied.

3. RESULTS

For this work our main goal is study of the system of chemical equations and clarification of assumptions. For that purpose it suffices to concentrate on steady state abundances in the presence of fixed gaseous concentrations of free C and O. During realistic evolution, the mass density declines and the temperature falls and carbon is slowly depleted from the gas. But even so the molecular abundances remain nearly in steady state, albeit one with a slowly evolving pattern. Early, above 2000 K, the thermal dissociation of the C_n molecules must be included in equation (15). But first we examine the solution in steady state at sufficiently low temperature that thermal dissociation is too slow to compete, doing this with the kinetic rates used by CLD99, which are listed in Table 1. These reference abundances provide a basis for comparison with those calculated using other rate choices. Equations (16) and (17) express that steady state for even-n and odd-n C_n molecules.

When the linear molecule becomes sufficiently long, spontaneous isomerization will thermally convert it to a ring. CLD99 chose a conservative $n = 24$ for this point, but the truth is not known and probably occurs also at significantly smaller n. Equation (15) should include destruction by an isomerization rate N_n/τ_{iso}, but we assume that rate to be small enough to not disturb the steady state abundances. The ringed isomer will be much less subject to oxidation, so that k_O declines markedly in value, whereas the associative properties of carbon are sufficiently robust to maintain a large value for k_C. With $k_C \gg k_O$, the abundance flattens (CLD99), resulting in the growth of macroscopic solids.

3.1. *Steady State with Standard Rates*

Figure 2 shows the steady state abundance ratios $N(C_n)/N(C)$ for a gas abundance ratio C/O = 1 and for standard reaction rates (Table 1). For reference numerical rates we choose $n = 10^{10}$ cm^{-3} (Fig. 1) for both free C and O (*squares*); however, examination of equations (16) and (17) shows that the solutions for $N(C_n)/N(C)$ depend only on the C/O ratio. The same standard result is obtained by our calculation if each have free density $n = 10^9$ cm^{-3}, for

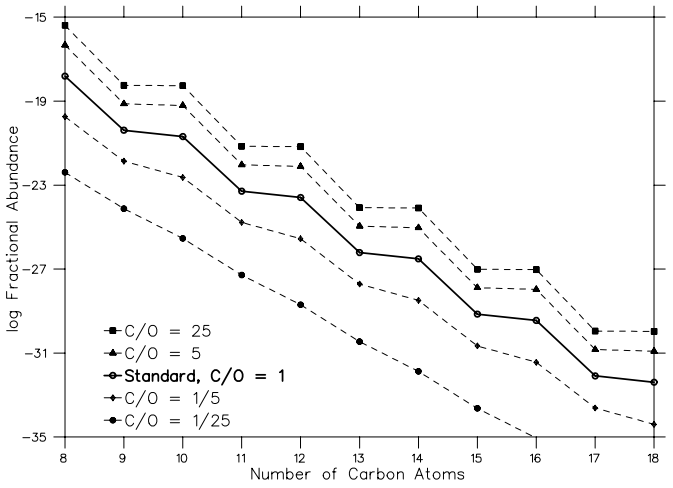

FIG. 2.—Steady state abundance ratios $N(C_n)/N(C)$ for a gas abundance ratio (C/O) = 1 is our standard calculation (*solid line*). For reference numerical rates we choose $n = 10^{10}$ cm^{-3} (Fig. 1) for both free C and O; however, examination of eqs. (16) and (17) shows that the solutions for $N(C_n)/N(C)$ depend only on the C/O ratio. Trends are shown for other values of C/O.

example. That is our first conclusion. It explains why the steady state pattern will change only slowly as the density declines. Both C and O decline during expansion, preserving their ratio. Because the molecular temperature falls as the density declines, moreover, the neglect of thermal dissociation becomes increasingly justified. What is plotted are the fractional abundances $N(C_n)/N(C)$ relative to free C atoms, which prior to condensation constitute roughly 99% of the total density of C atoms. We are not evolving the distribution as free C is depleted into solids in this work, but are content to present the chemical picture for fixed $N(C)$ and $N(O)$. The standard calculation takes ambient ratio C/O = 1, but results for C/O = 5, 1/5, and 1/25 are also shown for comparison. For the range shown (C_8 to C_{18} only) the fractional abundance drops steeply from about 10^{-18} for C_8 to about 10^{-31} for C_{18}.

Using the standard result in Figure 2, we can evaluate the production of C_6 by the $C_3 + C_3$ reaction, which was recommended by Curl (1993) for the laboratory production of fullerenes from C vapor. Taking the C-density maximum (Fig. 1) to be $n = 10^{10}$ cm^{-3}, the number density of C_3 becomes $n_3 = 10^{-2}$ cm^{-3}, so the rate (taken to be fast) of C_6 production is 10^{-14} cm^{-3} s^{-1}. But since the abundance of C_5 is $n_5 = 10^{-5}$ cm^{-3}, C_6 production by C association is 10^{-5} cm^{-3} s^{-1}, fully 9 orders of magnitude faster. The most competitive route is formation of C_5 by reactions between C_2 and C_3, which is only 1 order of magnitude slower than C association by C_4. By similar examinations we conclude that the supernova density during the dust epoch is too small for reactions of this type to compete with simple C association, as our equations assume.

Our result with C/O = 1 in Figure 2 is much smaller than the analogous result obtained by CLD99 in their Figure 2. The source of this difference has been hard to demonstrate owing to difficulty in recovering the CLD99 calculation. However, we suspect that their result was one of their calculations done with the fission rate constant $k_f = 0$ (no fission reactions possible), rather than one with fission included in the calculation. Our results show that $k_f = 0$ produces abundances very similar to those displayed by CLD99.

Role of isomerization.—It is evident from Figure 2 that the abundances of linear C_n will continue to decline with increasing n. The destruction rates for those linear molecules are just too great to allow a large abundance, even though they are much greater than thermal equilibrium would provide. How then are the large graphite solids to be grown? The key is the spontaneous isomerization of chains into monocyclic rings. Once that isomerization has occurred, the resulting ring is much more difficult to destroy either by fission or by oxidation. But carbon association can still proceed quite efficiently. These conclusions are essential to our overall picture, and to envision this we recommend that one imagine a ringed molecule injected into a gas of C atoms and O atoms. Our picture is that the C atoms will associate rapidly, whereas oxidation reactions, since they require bond breaking, will be much slower. In short, the carbon particle will grow larger rather than smaller as long as the abundant supply of free C atoms remains.

To appreciate such small abundances as those in Figure 2, consider that a fractional abundance near 10^{-20} is needed for the final micron-sized graphites if each is to contain 10^{15} C atoms (say) and if they are to constitute about 10^{-5} of all C by mass in the ejecta. This will require isomerization rates (for linear chains shown in Fig. 2) into ringed C that produce about 10^{-20} rings per C atom during roughly the first year of expansion. This might be achieved in many ways: a chain with an abundance of 10^{-20} isomerizing at the rate of 10^{-7} s^{-1} (that is, $\tau_{iso} = 10^7$ s) would yield 3×10^{-20} rings per year; or an abundance of 10^{-28} isomerizing at rate of 10 s^{-1} would also give 3×10^{-20} rings per year. We can find no quantitative knowledge of the isomerization rates for linear carbon chains in the literature; but we anticipate that the lifetime τ_{iso} against isomerization will decrease markedly with increasing length n. No theory or experiment known to us enables a firm identification of the chain length required for sufficiently rapid isomerization. It was for this reason that CLD99 simply assumed instantaneous isomerization at $n = 24$. That assumption was implemented by assuming that every carbon association by linear C_{23} results in ringed C_{24}. We have retained that assumption but note that isomerization of smaller, more abundant chains may produce more rings than does C_{24}. We therefore stress that work on those rates are important for supernova carbon condensation. Note that the abundances of Figure 2 do not include the depletion by the unknown isomerization rates, which were taken to be smaller than chemical destruction rates for purposes of generating this calculation.

The C/O *ratio.*—Another conclusion from Figure 2 is that different C/O ratios produce parallel trends, but reduction of C/O by a factor of 5 reduces the fractional abundances of C_n only by a factor near 100. Although this makes already small abundances even smaller, it is important to note that the abundances are not zero for C/O = 1/5. This observation emphasizes the kinetic non-LTE nature of this problem. Were one to instead calculate chemical thermal equilibrium at C/O = 1/5, the abundance of C_n would be vanishingly small! Second, even if C/O = 1/5, 10^{-20} rings may be produced per year from C_{14}, say, if its isomerization rate is near 10 s^{-1}. On the other hand, a carbon-rich C/O = 5, as may exist in the He-burning shell (see Fig. 1), produces no great increase of abundances in the supernova problem, whereas it is a huge facilitator in equi-

librium condensation calculations because when C/O = 5 one obtains free carbon in the equilibrium calculation, but carbon is maintained free by radioactivity in the supernova problem. For the C/O = 5 case, one must realize that oxidation by free oxygen still exists, because free oxygen exists even when it is less abundant than carbon. It is restored by disruption of CO. In this case oxidation is the net result of the radioactivity's maintenance of free oxygen even when O < C. So the radioactivity is essential to understanding of the chemical problem regardless of the relative abundances of C and O.

3.2. *Population Control*

More abundant nucleation does not imply more very large particles. The nuclei must not be too abundant or there will not exist enough C atoms to enable them to grow into large graphite particles. Kinetic destruction of the linear molecules controls their population, which in turn allows the rare ringed isomers to grow large before free C is depleted. Sufficient collisions to deplete all of the carbon do occur within an expanding supernova interior (see § 4). If the ringed nucleation molecules were as abundant as 10^{-12} per C, they could grow no larger than 1 μm (about 10^{12} atoms) before depleting all of the C into graphite. They would thus be too abundant to restrict the mass fraction to 10^{-5} for 1 μm particles. We call this principle "population control." We note that for this problem the ringed-isomer abundance near 10^{-20} appears to be about right.

When the linear molecule becomes sufficiently long, spontaneous isomerization will thermally convert it to a ring. The issue of the length required is significant, because the abundance C_n declines by about 0.01 from one even n to the next. Were the isomerization to occur at $n = 20$ rather than $n = 24$, the subsequent flat abundance level would be about 10^5 times increased, which would result in a corresponding increase in the abundances of the carbon solids that grow from the isomerization point, but at a cost to their final sizes if free C is depleted. The abundances and sizes of large solids are in this way determined by oxidative and fission population control of the linear C_n molecules, because their abundances in turn control the creation rate of ringed isomers.

An example of the possible application of population control may be seen in the comparison of the He-burning shell of Figure 1 (where C/O = 5) with the CO core (where C/O = 1/5). Figure 2 shows that whatever the identity of the most effective isomerizing chain (say, C_{14} just for definiteness), the number of ringed isomers per C atom is 2000 times greater in the helium-burning shell than in the CO core. This means that if depletion of carbon later becomes total, the final graphite grains will contain 2000 times fewer C atoms in the helium-burning shell. They will thus be about 10 times smaller in radius. This may explain the paucity of large graphites recovered experimentally from meteorites that were condensed within the helium-burning shell. If on the other hand the C does not deplete and the grain growth is collision limited, the lower C density in the He shell (Fig. 1) will again result in smaller particles there. This should be taken not so much as a firm prediction as an example of population control in action.

3.3. *Contrast with Thermal Equilibrium*

Many have found it hard to grasp the distinction between the steady state abundances for the C_n molecules and the unrestricted steady state that occurs in thermal and chemical equilibrium. With our results it becomes possible to clarify this with simple numerical observations. For definiteness focus on the time in the expansion of the CO core of a supernova when the C density has fallen to $N(\mathrm{C}) = 10^{10}$ cm^{-3}. Our calculation (Fig. 1) gives $N(\mathrm{C}_2) = 10^3$ cm^{-3} in steady state. The ratio $N_{\mathrm{eq}}(\mathrm{C}_2)/N(\mathrm{C})^2$ in chemical thermal equilibrium was discussed in § 2.1, where we showed that at $T = 2000$ K the ratio would be $N_{\mathrm{eq}}(\mathrm{C}_2)/N(\mathrm{C})^2 = 2.2 \times 10^{-11}$. Using $N(\mathrm{C}) = 10^{10}$ gives the ratio

$$\left[\frac{N(\mathrm{C}_2)}{N(\mathrm{C})}\right]_{\mathrm{eq}} = 0.22 , \tag{19}$$

where the subscript "eq" reminds us that it applies to true equilibrium. By contrast, the solution obtained in steady state (Fig. 1) is

$$\left[\frac{N(\mathrm{C}_2)}{N(\mathrm{C})}\right]_{\mathrm{ss}} = 10^{-7} \tag{20}$$

fully 6 orders of magnitude smaller, a result that can be seen readily by equating the creation of C_2 with its main mode of destruction, oxidation: namely,

$$k_{\mathrm{C}} N(\mathrm{C})^2 = k_{\mathrm{O}}(\mathrm{C}_2) N(\mathrm{C}_2) , \tag{21}$$

and by noting $k_{\mathrm{C}} = 10^{-17}$ and $k_{\mathrm{O}} = 10^{-10}$. The result follows. Although this sounds as if one obtains *more* C_2 in the state of thermal and chemical equilibrium, that impression is deceptive. In thermal equilibrium the free abundance of carbon $N(\mathrm{C})$ at $T = 2000$ K would be tiny, not $N(\mathrm{C}) = 10^{10}$ cm^{-3}. The carbon would be overwhelmingly bound in CO molecules, as we discussed previously. In that case the actual equilibrium ratio would be

$$\left[\frac{N(\mathrm{C}_2)}{N(\mathrm{C})}\right]_{\mathrm{eq}} = 2.2 \times 10^{-11} N(\mathrm{C})_{\mathrm{eq}} . \tag{22}$$

It is the small size of $N(\mathrm{C})_{\mathrm{eq}}$ that makes thermal-equilibrium abundances very small. By contrast, the steady state solution has the luxury of abundant free carbon owing to the nonthermal destruction of CO.

The distinction can equally well be seen from the balances of reaction rates. In chemical thermal equilibrium, every reaction occurs at the same rate as the inverse of that reaction. That is a condition that is not true in simple steady state. Thus the rate of radiative creation of C_2, which is $10^{-17}(10^{10})^2 = 10^3$ cm^{-3} s^{-1}, should be exactly balanced in thermal equilibrium by the thermal photodestruction rate of C_2. Section 2.1 showed its lifetime to be 2.2×10^6 s at $T = 2000$ K, so thermal disruption of C_2 occurs only at the rate $N(\mathrm{C}_2)/2.2 \times 10^6 = 10^3/2.2 \times 10^6 = 4.5 \times 10^{-4}$. This thermal dissociation rate of C_2 fails by a factor near 10^6 to balance the creation of C_2 by association. The destruction rate of C_2 is instead dominated by oxidation, as the average molecule lives only 1 s before destruction by oxidation.

The gross mismatch between chemical thermal equilibrium and the steady state set up by reaction kinetics serves as a vivid illustration of the supernova conditions insofar as the condensation of carbon is concerned. Owing to the radioactive destruction of CO molecules, the free carbon density $N(\mathrm{C})$ remains very high, much more than thermal equilibrium would ever allow near 2000 K. At that temperature all of carbon has normally reacted with some-

thing and, except in radioactive supernovae, remains bound. It is the large free carbon density at low temperature that drives carbon condensation in the radioactive supernova.

3.4. *A* CO *Diagnostic of Core Collapse to a Black Hole*

We point to a significant diagnostic of a massive-star supernova whose core collapses to a black hole. Fallback would swallow most of the radioactive ^{56}Co, ^{57}Co, and ^{44}Ti created in the alpha-rich freezeout of shocked matter. In this case the radioactive environment will be diminished by a large factor, with the result that CO is not dissociated as rapidly. The steady abundance of CO will increase in proportion. Such a core-collapse supernova will eject a huge mass of CO molecules in comparison with the mass ejected from SN1987A. Observation of such a phenomenon would diagnose (or confirm other observations) that the core has collapsed to a black hole, or at least that the radioactivity fell back onto the neutron star.

3.5. *Survey of Reaction Rates*

Because supernova condensation is controlled by kinetic rates it is of interest to examine which reaction rates are the most critical for the outcome. In what follows we increase or decrease all of the reaction rates of specified type. For example, we first change all fission rates by the same factor.

Fission rates.—Fission rates are very important. We have taken their rates to be as fast as oxidation in the destruction of the even-n chains. Figure 3 shows the standard reference calculation as well as a comparison result if the fission rate for even n is slowed from the fast $k_f = 10^{-10}$ to 10^{-11} cm^3 s^{-1} and then even more to 10^{-12} cm^3 s^{-1} with all other rates held at the reference values. It is clear that despite the continued rapid destruction by oxidation, the abundances increase greatly (about 15 orders of magnitude for C_{20}) by the slowdown factor (100) in these even-n fission rates.

The standard calculation has taken the identical fission rate for each C_{2n} molecule, but we examine whether individual variations from that rate are significant, and if so, which fissioning molecule has largest impact on the overall problem. Table 3 shows selected results illustrating the comparative significance of the rate of fission of C_{2n} on the steady state abundances. Each value of k_f for even n is, in turn, decreased by a factor of 10 to $k_f = 10^{-11}$ cm^3 s^{-1}, and the resulting enhancement of the steady state abundances is listed for three characteristic molecules: C_4, C_{10}, and C_{20}. The results are somewhat difficult to understand at first glance. Easiest to understand is that the 10-fold smaller fission rate for C_4 (fourth column) results in larger abundance for C_4 by a factor of 1.9. This increase reflects the smaller destruction rate of C_4, which is destroyed equally by fission and oxidation in the standard case but primarily by oxidation when its fission rate is reduced 10-fold; whence the ratio of total destruction rates is just 2.0/1.1 = 1.82, most of the factor of 1.9 by which the C_4 abundance has increased. But one also notices that every C_n heavier than the molecule whose fission rate is reduced is increased by the same factor, not just the one having its fission rate reduced. This is because the linear equation set maintains the identical ratios for heavier molecules. For example, reduction of k_f for C_6 (sixth column) increases the abundance of C_{10} and C_{20} by identical factors of 9.79. The abundances of C_{10} and C_{20} are increased by an almost identical factor if the reduction of fission rate occurs at either C_8 or C_{10}, a factor of 9.81 each. This can be understood as a feedback that attempts to maintain the abundances below the one having reduced fission at the values that they took on in the standard calculation, but doing so requires a factor of 10 increase in abundance of that C_n molecule whose fission rate is being reduced to offset the factor of 10 reduction of its k_f. It is helpful to recall from Figure 2 that in the standard calculation the abundance falls by about 2 orders of magnitude for each increase of n by 2. Thus the factors shown in Table 3 as abundances relative to standard show that the fall is reduced from 2 orders of 10 to just 1 by the reduction of k_f by a factor of 10.

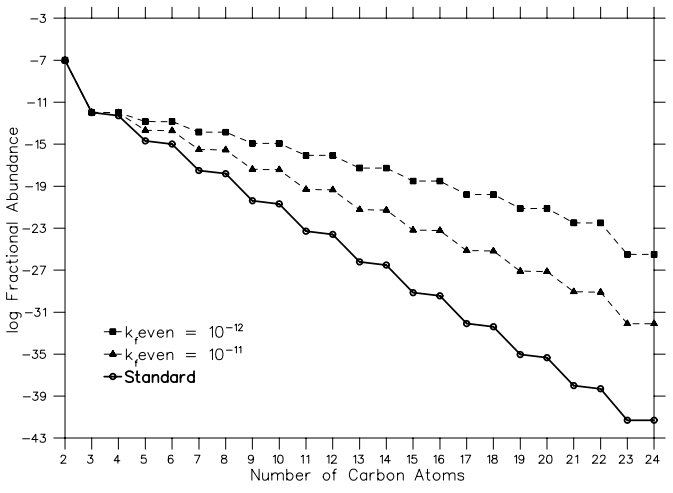

FIG. 3.—Standard reference calculation as well as a comparison result if the fission rate for even n is slowed from the fast $k_f = 10^{-10}$ to 10^{-11} cm^3 s^{-1} and then even more to 10^{-12} cm^3 s^{-1} with all other rates held at the reference values. It is clear that despite the continued rapid destruction by oxidation, the abundances increase greatly (about 15 orders of magnitude for C_{20}) by the slowdown factor (100) in these even-n fission rates.

TABLE 3

ENHANCEMENTS OF C_4, C_{10}, AND C_{20} WHEN $k_f(n)$ IS REDUCED BY A FACTOR OF 10

	n				
SPECIES	4	6	8	10	12
C_4.....	1.90	0.999	1	1	1
C_{10}.....	1.90	9.79	9.81	9.81	1
C_{20}.....	1.89	9.79	9.81	9.81	9.81

Table 4 shows selected results illustrating the comparative significance of the identity of the dominant channel for fission by one molecule, taken for illustration to be C_{10}, on the steady state abundances of C_4, C_8, C_{10}, C_{12}, and C_{20}. The numbers entered are the enhancement factors for that

TABLE 4

FISSION OF C_{10} (100% IN C_m)

	LARGER FRAGMENT m			
SPECIES	6	7	8	9
C_4.....	1	1	1	1
C_8.....	0.999	1.00	1.00	0.999
C_{10}.....	0.750	0.751	0.751	114.8
C_{12}.....	0.750	0.751	0.751	114.2
C_{20}.....	0.750	0.751	0.751	112.2

abundance if the larger fragment is C_m (in which case the smaller fragment must be C_{11-m}). For this test each value of k_f is maintained at $k_f = 10^{-10}$ cm^3 s^{-1}, but that standard fission rate is focused successively into a single specific channel, $C_m + C_{11-m}$, with m being the larger fragment, instead of being distributed equally among all channels (our standard assumption). For each specific choice of the fission channel (as identified by the larger fragment) the resulting enhancement of the abundance is listed for those five molecules. One notices that concentrating fission into any channel but the heaviest has little effect on the abundances, whereas fission concentrated into the heaviest channel (C_9) results in significant enhancement factors for each molecule heavier than C_9.The latter increase by an equal factor to maintain constant ratios above $n = 9$, and the size of that enhancement is determined by a surprisingly large reduction of the effective destruction rate of the fissioning molecule, which comes about because oxidation is not really effective destruction of C_{2n} since the resulting odd-n molecule overwhelmingly associates with a C atom to return to the fissioning nucleus. Concentrating fission into the heaviest fragment possible is equivalent to endowing fission with effectively the same result as oxidation, that is, ineffective as a destruction mechanism.

Figure 4 repeats Figure 3, but with one different curve for which the standard fission rate for each even-n molecule is concentrated entirely into its largest fragment. It can be seen that the result increases the abundances almost to the level they would have were fission neglected entirely ($k_f = 0$). We thereby demonstrate that the fission reaction branchings cluster into two groups whose relative size is significant: namely, fission into the largest fragment $C_{max} + C_2$, and fission into all other channels. Because these branchings are poorly known, it is to be hoped that the theory of this reaction and measurements can guide this interesting application.

Carbon-association rates.—The carbon-association rate with linear C_{2n} is also important, but also unknown. We have taken the C-association rate to be small for even C_{2n}, only 1/1000 of the fission rate, because the fast fission does not allow time for the C association to radiatively stabilize. Here we explore the sensitivity to its actual value. Results are shown in Figure 5. Increasing k_C for even n from 10^{-13} to 10^{-11} cm^3 s^{-1} while holding other rates fixed vastly increases the abundances. Increasing association 10-fold to $k_C = 10^{-12}$ cm^3 s^{-1} is almost identical to slowing the fission rate by a factor of 10 (see Fig. 3). This similarity shows that it is the branching ratio k_C/k_f for even-n molecules that governs the abundances as long as only modest variations are involved. But further increase to $k_C = 10^{-11}$ cm^3 s^{-1} results in huge abundance increase. Even though that association rate remains smaller than both destruction rates of C_{2n} by a factor of 10, it produces a much flatter abundance curve. With such a flat curve, the doubling of molecule number accomplished by each fission plays an important new role in the steady state abundances, which become even greater than those that would obtain were there no fission at all! That is, fission actually increases the abundance of each C_n for even-n association rates as large as $k_C = 10^{-11}$ cm^3 s^{-1}. Inefficient population control resulting from that large value of k_C would, however, create too many particles (unless isomerization to ringed structure is much slower than expected), resulting in a large number of small graphite grains rather than a smaller number of large ones (as observed).

Figure 5 includes one case simultaneously altering k_C and k_f for the even-n chain molecules. The standard value of k_C is increased by a factor of 30 to $k_C = 3 \times 10^{-12}$ cm^3 s^{-1} while the fission rate is reduced 10-fold to $k_f = 10^{-11}$ cm^3 s^{-1}. Each change separately increases each abundance moderately, but acting together they produce a dramatic increase in abundance.

We demonstrate in Figure 6 that the assumption of fast k_C for the odd-n linear chains C_{2n+1} is not so crucial. This is because C association dominates destruction of odd-n molecules; decreasing all such rates would therefore increase their abundances but for its also decreasing the creation rates of the even-n C_{2n} by compensating factors. These compensate within the general decline. Figure 6 illustrates that

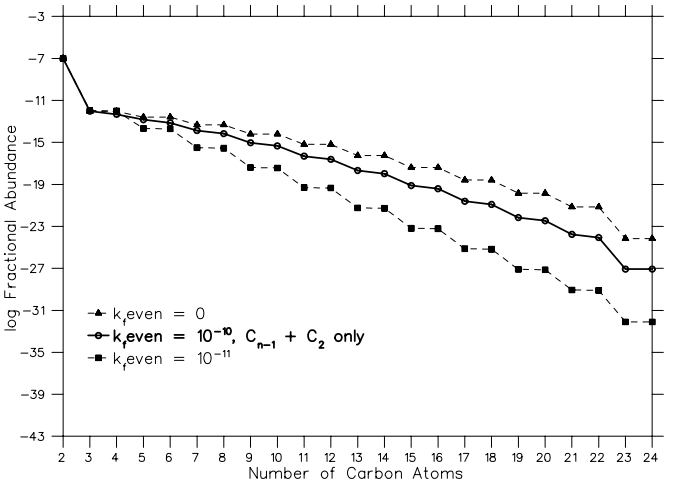

FIG. 4.—Fast fission into only the largest fragment. This repeats for reference the effect of decreased fission rates as in Fig. 3, but with one added curve (*solid line*) for which the standard fission rate for each even-n molecule is retained at its standard fast value but concentrated for each reaction entirely into its largest fragment. It can be seen that doing so increases the abundances almost to the level they would have were fission neglected entirely ($k_f = 0$). Absence of fission reactions ($k_f = 0$) results in abundances similar to those obtained by CLD99.

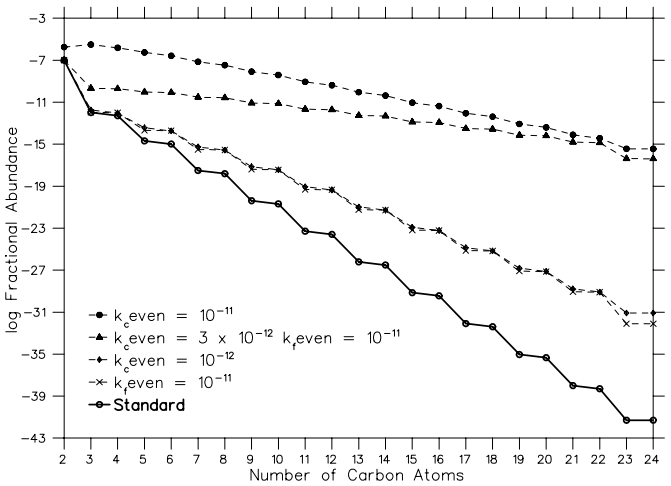

FIG. 5.—Increasing k_C for even n to 10^{-11} cm^3 s^{-1} while holding other rates fixed vastly increases the abundances. Increasing association 10-fold is almost identical to slowing the fission rate by a factor of 10 (see Fig. 3). We also include one case where k_C and k_f are altered simultaneously for the even-n chain molecules. The standard value of k_C is increased by a factor of 30 while the fission rate is reduced by a factor of 10.

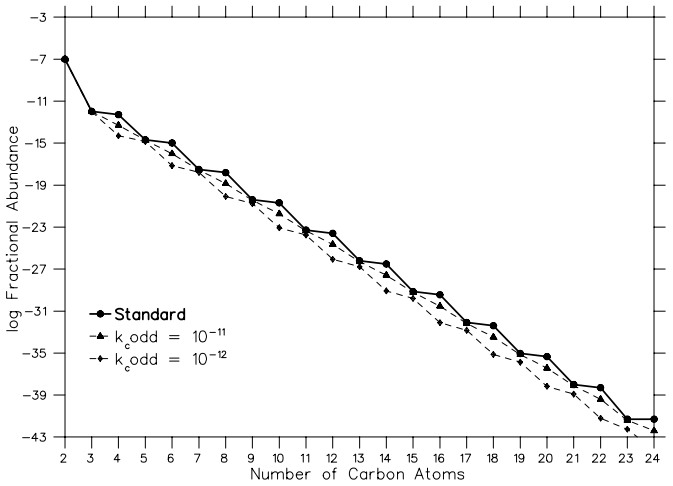

FIG. 6.—Changes of the fast k_C for the odd-n linear chains C_{2n+1}. This weak dependence arises because C association dominates destruction of odd-n molecules.

even a 2 order of magnitude decrease of k_C leaves the same general decline in abundances, although it does smooth out the odd-even effect.

Oxidation rates.—We have taken the oxidation rate to be fast for even-n chains and to be $k_O = 10^{-13}$ cm^3 s^{-1} for odd-n chains, which is much smaller than the C-association rate for odd n. If the oxidation rate for odd n is less than the C-association rate, its exact value is not a critical unknown. We find that increasing the value of k_O by even a factor of 100 does not alter the abundance curve. Figure 7 shows the factor by which the abundances are changed by plotting the ratio of the abundance of C_n after the alteration of rates to its value with the standard rates. Only a very small change (*open circles*) results from a factor of 50 increase of k_O. Note that the standard calculation is not shown in Figure 7, but it would be a horizontal line at unity. Other results are plotted in their ratio to the standard result.

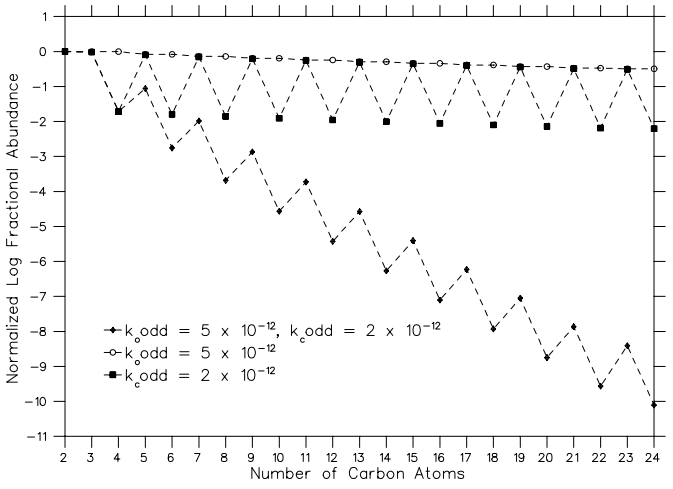

FIG. 7.—Effect of oxidation rates. The factor by which changes of oxidation rates change the abundances are shown by plotting the ratio of the abundance of C_n after the alteration of rates against its value using the standard rates. Only a very small change (*open circles*) results from a factor of 50 increase of k_O. Note that the standard calculation is not shown but would be a horizontal line at unity. Also shown as filled squares in Fig. 7 is the change of abundances caused by the reduction of odd-n k_C by a factor of 50, as well as that change coupled with the increase of oxidation by a factor of 50.

Also shown as solid squares in Figure 7 is the reduction of odd-n k_C by a factor of 50. When this change alone is made, the odd C_{2n+1} are not affected (because although they are destroyed 50 times more slowly, they are also produced 50 times more slowly by the decreased abundance of the even C_{2n}, which are themselves reduced by a factor of 50 because their production has been decreased by that factor). However, simultaneous large increase of k_O and decrease of k_C would impact these results more dramatically. The bottom curve in Figure 7 illustrates this with k_O increased by a factor of 50 to $k_O = 5 \times 10^{-12}$ cm^3 s^{-1} and association slowed by the same factor of 50 to $k_C = 2 \times 10^{-12}$ cm^3 s^{-1}. Such modification makes oxidation slightly faster than C association for odd-n molecules, with the evident drop in chain abundances in Figure 7. C_{20} is now about 10^{-9} of the standard result. Identification of the significant kinetic rates is clouded by such examples where changing two rates produces a much bigger effect than could be guessed naively from the individual impact of each change separately.

4. GROWTH OF LARGE GRAPHITE SOLIDS

This paper has calculated the abundances of the linear-chain molecules and their dependences on collisional rates. We have also discussed the importance of isomerization rates in determining the creation rate of ringed isomers. We conclude by summarizing how these lead to the macroscopic particles contained in the interstellar medium and trapped within meteorites.

The fractional abundance 10^{-20} may sound very small, but CLD99 showed that it is not too small for what is observed of supernova graphite particles. From the concentration of supernova graphite in carbonaceous meteorites, it can be concluded (Clayton et al. 1997) that the mass fraction of all interstellar carbon that had been ejected from supernovae as large graphite particles is near 10^{-5}. Since 10 μm particles contain 10^{15} C atoms, their number fraction should be no greater than 10^{-20}, comparable to the number fractions that can be generated by our calculations, depending on the isomerization rate of linear molecules into rings.

Consider first the fate of a ring molecule created by an isomeric transition of linear C_n. We expect carbon to associate rapidly with such ring molecules. For an associative rate coefficient $k_C = 10^{-10}$ cm^3 s^{-1} and carbon density near 10^{10} cm^{-3}, the mean time between successive captures is of order $1/k_C n_C = 1$ s. For simplicity assume that condensation begins at that time t_0. But because the C density is declining owing to expansion as $n_C(t) = n_C(t_0)(t/t_0)^{-3}$, the growth rate at each value of n for a chosen particle is also declining. If k_C is taken to be constant and if $n_C(t)$ declines only by expansion without depletion, the equation

$$\frac{dn}{dt} = k_C n_C(t) = 1 s^{-1}(t/t_0)^{-3} \quad (23)$$

can be integrated from a starting time t_0 to infinite time (complete dispersal). Doing so yields for the limiting size

$$n_{max} = \frac{t_0}{2} = 10^7 \quad (24)$$

if we assume that the process begins in roughly half a year ($t_0 = 2 \times 10^7$ s, say, as in Fig. 1). With such assumptions we expect a fairly flat fractional abundance out all the way to

$n = 10^7$. CLD99 called this the "flat model" (although that name is not especially suitable). This n_{max} is already a particle of diameter near 0.1 μm, about one-tenth of the size of the large supernova graphite particles studied in the laboratory (Amari & Zinner 1997). But it is well short of the $n = 10^{12}$ atoms required by a 1 μm grain.

As CLD99 pointed out, macroscopic carbon grains increase in geometric area, so that k_C should increase in proportion. This assumption is similar to the assumption made long ago (Clayton & Wickramasinghe 1976; Clayton 1979) in their exploration of particle growth in an explosively expanding medium. They used $k = s\pi a^2 v_{th}$, where s is the sticking probability, a is the radius of the particle, and v_{th} is the mean thermal speed of the C atoms. Their integration analytically gives a_{max} near 100 μm for unit sticking probability, considerably greater than the micron-sized graphites from supernovae found in the meteorites.

To achieve a size in excess of 0.1 μm within the time available, k_n(C) must grow with n, as may occur because of the larger surface area of the macroparticles. CLD99 called this growth of k_C with size a "growth model," which assumes $k_n(C) \propto n^{2/3}$ for $n > 24$ and which produces a much larger population of the micron-sized dust particles by increasing the final size reached. Figure 3 in CLD99 showed their result for the fractional mass in decadal size bins: namely, that it increases with particle size. It predicts that the greatest mass fraction resides in the largest graphite particles. This may account for the meteoritic observations that most of the supernova graphite seems to be large (0.8–20 μm) particles with mass fractions of order 10^{-5} (Clayton et al. 1997). We can estimate the final sizes if we assume that the C density declines owing only to expansion. The growth of particle size will instead be

$$\frac{dn}{dt} = k_C n_C(t) = 1 s^{-1} \left(\frac{n}{24}\right)^{2/3} \left(\frac{t}{t_0}\right)^{-3} , \quad (25)$$

which can also be integrated to yield a final size

$$n_{max} = \left(\frac{t_0}{50}\right)^3 = 6 \times 10^{16} . \quad (26)$$

This is a larger graphite SUNOCON (40 μm) than any yet found within meteorites, which are 0.8–20 μm. Though this calculation is both rough and optimistic, it confirms the result of Clayton & Wickramasinghe (1976) and Clayton (1979): namely, very large graphites may grow in a supernova if the gaseous C is not depleted. Whether the C is depleted depends upon the number of grain nuclei (population control).

Oxides.—These same principles, when mirrored, also enable oxides to grow within supernova gas having C > O. Possible evidence of such an oxide grain has been reported (Choi, Huss, & Wasserburg 1998) in the form of corundum (Al_2O_3) grains from the Semarkona meteorite with a large excess of ^{18}O. This large ^{18}O excess exists in the He-burning shell of the supernova, which is also the only supernova shell having C > O (Clayton 1981), a composition that would otherwise be expected under thermochemical equilibrium to prevent condensation of an aluminum oxide solid by locking up the oxygen in CO molecules. We stress that within supernovae the relative abundance of C and O does not determine whether carbon or oxide grains may condense, as it does in thermal equilibrium. Indeed, the maintenance of free O atoms in that zone may conspire to facilitate the growth of Al_2O_3 even while carbon is simultaneously condensing.

Fullerenes.—Does this model lead to fullerenes? With our assumption of rapid carbon association for ringed molecules, an isomeric ring created when the free C density is large will be quickly converted to a large graphite particle. That bypasses fullerenes. The situation might seem more promising near the end of the condensation, when both depletion and expansion yield a small density of free carbon. The subsequent growth of rings made at this time will be collision limited. Final sizes for them may be appropriate for fullerenes. But examination of our Figure 2 reveals that the mass fraction of carbon in such fullerenes would then be small.

A more promising approach questions the chemical assumptions. To obtain a large mass fraction in fullerenes seems to require that a reason be found to halt C-association growth for certain fullerenes—"magic numbers"—that is, to create them early when n_C is still large but have them withdraw from further growth, as if relatively inert. Exactly this has been described by Curl (1993), who notes that buckminsterfullerene has no weak point for chemical attack, all C atoms being identical and equal. Though slightly less true for other fullerenes, this difficulty of chemical attack may leave abundant fullerenes as "survivors" of the otherwise upward associative flow. A simple picture might have a C atom sticking (weakly) to a fullerene then being quickly removed thermally or by oxidation. We note that fullerenes have been reported in carbonaceous meteorites (Becker, Bunch, & Allamandola 1999), although some controversy has surrounded the reports. We regard this "survivor mechanism" as a credible source for abundant supernova fullerenes. Let it be clear that most of the association flow through C_{60} does not pass through buckminsterfullerene but rather through a higher energy isomer of 60 atoms. Only if isomeric transition to the fullerene occurs within the few seconds available before the next C association does the fullerene remain as an inert survivor; Hunter et al. (1994) and von Helden et al. (1993) have described the annealing of rings into fullerenes.

5. SUMMARY

We have presented this scenario for the condensation of large graphite grains within the O-rich CO core of Type II supernovae. The radioactivity produces fast particles that directly or indirectly disrupt the CO molecule, leaving ample free C and O. The C atoms associate into linear chains of rapidly dropping abundance with length n. Their population is controlled by the destructive oxidation and fission reactions that proceed rapidly on even-n chains.

The key dynamic feature is the isomerization of a linear C_n chain into a ringed C_n isomer. From that moment on, carbon association remains fast, but the destructive oxidation and fission reactions become much slower. This enables steady capture of C atoms until larger sizes are achieved. First bicyclic and tricyclic rings may anneal to fullerenes (Hunter et al. 1994; von Helden et al. 1993). All ringed clusters nucleate the macroscopic graphite grains, which contain up to $n = 10^{15}$ atoms in the SUNOCONs found within meteorites. The C-association rate increases owing to the increasing geometric size of the macroparticle, concentrating the condensed-C mass fraction into the largest sizes that can be achieved during the few years of expansion and condensation.

This sequence effectively identifies the nucleation for the growth of macroscopic grains. It alleviates the need to admix gases from elsewhere in the attempt to maintain a C/O ratio greater than unity, because free carbon exists anyhow. This nucleation theory replaces (in the supernova) the chemical equilibrium nucleation theory.

We have surveyed the dependence of this result on the unknown kinetic reaction rates involved. Key among these are the ratio of C association to C-induced fission for the even-n linear chains; the ratio of fission into the largest-fragment channel to that into all other channels; and the absolute value of the C-association rate for the few-n molecules, which requires that they capture first and radiatively stabilize later. Above all, no large grains would be grown but for the isomerization into ringed molecules, the lifetimes for which become key astrophysical data, still unknown.

The results are of high significance for the optical properties of young supernova remnants (1–10 yr old) and for the supernova astrophysics that can be found written in presolar graphite (and SiC) grains that demonstrably condensed within supernovae (Clayton et al. 1997).

This 4 year project owes thanks to many. Weihong Liu and Alex Dalgarno greatly contributed to the development of the quantitative picture and its key chemical steps. Eric Herbst and Ryan Bettens offered very helpful advice and data concerning the molecules. Lih-Sin The helped with the computations. Craig Wheeler provided Figure 1 within a stimulating numerical study of CO formation within a model of SN1987A. This work has been supported by the Cosmochemistry program of NASA and by NSF grant AST 98-19877.

REFERENCES

Amari, S., & Zinner, E. 1997, in Astrophysical Implications of the Laboratory Study of Presolar Materials, ed. T. J. Bernatowicz & E. Zinner (Woodbury: AIP), 287
Bates, D. R. 1983, ApJ, 267, L121
Becker, L., Bunch, T. E., & Allamandola, L. J. 1999, Lunar Planet. Sci. Conf., 30, 1805
Bernatowicz, T. J., Cowsik, R., Gibbons, P. C., Lodders, K., Fegley, B. J., Amari, S., & Lewis, R. S. 1996, ApJ, 472, 760
Bernatowicz, T., & Walker, R. M. 1997, Phys. Today, 50, 26
Bettens, R. P. A., & Herbst, E. 1995, Int. J. Mass Spectrom. Ion Processes, 149/150, 321
———. 1996, ApJ, 468, 686
———. 1997, ApJ, 478, 585
Bettens, R. P. A., Lee, H., & Herbst, E. 1995, ApJ, 443, 664
Choi, B., Huss, G. R., & Wasserburg, G. J. 1998, Meteoritics Planet. Sci. A, 33, 32
Clayton, D. D. 1975, Nature, 257, 36
———. 1978, Moon Planets, 19, 109
———. 1979, Ap&SS, 65, 179
———. 1981, Lunar Planet. Sci. Conf., 12, 151
Clayton, D. D., Amari, S., & Zinner, E. 1997, Ap&SS, 251, 355
Clayton, D. D., Colgate, S. A., & Fishman, G. J. 1969, ApJ, 155, 75
Clayton, D. D., Liu, W., & Dalgarno, A. 1999, Science, 283, 1290 (CLD99)
Clayton, D. D., & The, L. 1991, ApJ, 375, 221
Clayton, D. D., & Wickramasinghe, N. C. 1976, Ap&SS, 42, 463
Colgate, S. A., & McKee, C. 1969, ApJ, 157, 623
Curl, R. F. 1993, Philos. Trans. R. Soc. London, 343, 19
Freed, K. F., Oka, T., & Suzuki, H. 1982, ApJ, 263, 718
Gearhart, R. A., Wheeler, J. C., & Swartz, D. A. 1999, ApJ, 510, 944
Gupta, S., & Meyer, B. S. 2001, Phys. Rev. C, in press
Herbst, E., & Dunbar, R. C. 1991, MNRAS, 253, 341
Herbst, E., Lee, H. H., Howe, D. A., & Millar, T. J. 1994, MNRAS, 268, 335
Hoppe, P., Strebel, R., Eberhardt, P., Amari, S., & Lewis, R. S. 1996a, Science, 272, 1314
———. 1996b, Geochim. Cosmochim. Acta, 60, 883
Hunter, J. M., Fye, J. L., Roskamp, E. J., & Jarrold, M. F. 1994, J. Phys. Chem, 98, 1810
Lepp, S., Dalgarno, A., & McCray, R. 1990, ApJ, 358, 262
Liu, W., & Dalgarno, A. 1994, ApJ, 428, 769
———. 1995, ApJ, 454, 472
———. 1996, ApJ, 471, 480
Liu, W., Dalgarno, A., & Lepp, S. 1992, ApJ, 396, 679
Lodders, K., & Fegley, B. J. 1997, ApJ, 484, L71
Nittler, L. R., Amari, S., Zinner, E., Woosley, S. E., & Lewis, R. S. 1996, ApJ, 462, L31
Pascoli, G., & Polleux, A. 2000, A&A, 359, 799
Sharp, C. M., & Wasserburg, G. J. 1995, Geochim. Cosmochim. Acta, 59, 1633
Terzieva, R., & Herbst, E. 1998, ApJ, 501, 207
Travaglio, C., Gallino, R., Amari, S., Zinner, E., Woosley, S., & Lewis, R. S. 1999, ApJ, 510, 325
von Helden, G., Gotts, N. G., & Bowers, M. T. 1993, Nature, 363, 60
Weltner, W., & Van Zee, R. J. 1989, Chem. Rev., 89, 1713
Wooden, D. H. 1997, in AIP Conf. Proc. 402, Astrophysical Implications of the Laboratory Study of Presolar Materials, ed. T. J. Bernatowicz & E. Zinner (Woodbury: AIP), 317
Woon, D. E., & Herbst, E. 1996, ApJ, 465, 795